



Oxa-bridged Donor-Acceptor systems containing Triazine core for Dye Sensitized Solar Cell Application

Suma Chemban Subramanian, Maheshkumar Madathikudy Velayudhan,
Manoj Narayanapillai*

Department of Applied Chemistry, Cochin University of Science & Technology, Kochi-22, Kerala, India
(*E-mail: manoj.n@cusat.ac.in)

Abstract: Novel Donor-Acceptor systems of D- π -A-A type incorporating electron deficient triazine moiety as a non-conjugating π -spacer/acceptor with rhodanine acetic acid (DTOP-RHA), barbituric acid (DTOP-BA) or thiobarbituric acid (DTOP-TBA) as anchoring acceptor groups have been synthesized. Diphenylamine is used as the donor moiety and the role of the anchoring group and the π spacer are studied. These dyes are tested as sensitizers in the dye sensitized solar cells. The efficiencies obtained were low compared to the standard dye N719 under identical experimental conditions. This is attributed to the short wavelength absorption characteristics of the dyes as well as the larger energy gap between the LUMO of the dyes and the TiO₂ conduction band.

Key Words: - TiO₂, 1,3,5-Triazine, Donor-Acceptor systems, Electron transfer, DSSC.

INTRODUCTION

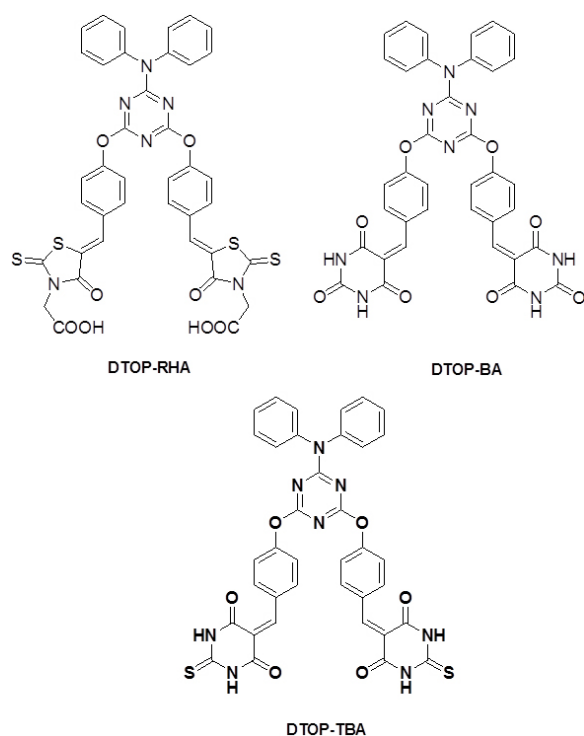
Among emerging photovoltaic device technology, DSSCs and Perovskite cells find an important place. Regarding the efficiencies of these types of cells DSSC report a highest efficiency of 11.9 % and Perovskite cells report 22.1% [1-2]. In recent years, dye-sensitized solar cells (DSSCs) have engrossed much interest due to their potential advantages like cost effective, flexible and straight forward device fabrication [3-9]. Dye sensitized solar cells based on coordination complexes with heavy metal ions are considered as the most efficient device, but cannot be used for large scale applications due to the limited resources and high cost [10-13]. The challenge is open to develop new systems using cost effective materials and promising photoconversion efficiencies. Use of organic D- π -A dyes are one such option with promising results. Most widely studied D- π -A systems include triphenylamine as the donor and cyanoacrylic acid moiety as acceptor [14-17]. Different π spacers with planar configuration, effectively improve the electron-transportation from donors to acceptors and results in significant change in overall photovoltaic performances

[18-20]. Electron deficient heterocyclic structural units such as thiazole, triazine, cyanovinyl, cyano- and fluoro-substituted phenyl groups etc., have been used as the π bridges in the D- π -A-A systems. They exhibit several advantages over the straight D- π -A systems, with significantly changes the molecular energy levels, absorption characteristics and finally the overall photovoltaic performance [21, 22]. 1,3,5-triazine have been used as a building block for the synthesis of D- π -A-A systems as dyes in DSSC. In recent literature triphenylamine or porphyrins have been used in a similar solar cell design with cyanoacrylic acid as the acceptor as well as the anchoring groups. Here we report a series of dyes where diphenylamine as the donor unit and rhodanine acetic acid, barbituric acid or thiobarbituric acid linked to 1,3,5-triazine as the π - acceptor unit.

In simple valence bond terms, when there are two substituents on a benzene ring which are *meta* to each other the possibility of conjugation of π orbitals of one with the other is not possible due to the absence of resonance form of the benzene ring supporting such conjugation. This gives us the possibility of designing dyes having intramolecular charge transfer states, in which Donor and Acceptor moieties are separated in space and thus increase

the length of the charge separation in comparison to directly coupled systems. But such charge separation is useful only when the lifetime of such intramolecular charge separated state is long enough to permit subsequent electron transfer cascade when they are used as dyes and light harvesting systems in photo-voltaic or photo-electrochemical systems. The lifetime of the ICT state depends on the free energy of the back electron transfer regenerating the ground state [23, 24].

Keeping these ideas in mind we have designed dye molecules of D- π -A type triads with 1,3,5-triazine as the first acceptor and as the core bridging π unit. Donor moiety chosen was diphenylamine. Rhodanine acetic acid, barbituric acid and thiobarbituric acid were chosen as the second acceptors with varying electron affinity and binding ability to TiO₂ surface. In the current paper we report the synthesis, photophysical and photoelectrochemical properties of these three D- π -A type triads. (Scheme1).



Scheme 1. Structures of the compounds

EXPERIMENTAL SECTION

General Techniques

All reagents were obtained from Sigma-Aldrich or Spectrochem at the highest purity and used without further purification. All reactions were carried out at anhydrous conditions and under air/nitrogen

atmosphere. Dimethyl formamide (DMF) and dichloromethane were distilled and dried over molecular sieves (3 Å X 1.5 mm). The ¹H and ¹³C NMR spectra were recorded at 400 MHz Bruker Avance III FT-NMR spectrometer in CDCl₃ or DMSO-d₆. Elemental analysis was performed using Elementar Systeme (Vario EL III) CHN analyser. Molecular mass was determined by electron impact (EI) method on GC-MS (Agilent GC-7890A, Mass-5975C) or ESI on Waters Model e 2695 ESI MS. UV-Vis absorption spectrometry of the dyes in dry DMF solutions were carried out on Thermo Evolution Model 201. All melting points were uncorrected and determined on a Neolab melting point apparatus. FT-IR spectra were recorded using Jasco Model 4100 FT-IR spectrometer. The materials used for DSSC fabrication such as the conducting fluorine Indium Tin Oxide plates (7 Ω/sq), Platisol T, N719 dye, Iodolyte HI-30 and naocrystalline Titania Paste (Ti-Nanoxide) were purchased from Solaronix. Separation and purification of compounds were done by column chromatography using either silica gel (Spectrochem, 60-120 mesh) or neutral alumina (Spectrochem).

Synthesis and Characterization.

Synthesis of 4,6-dichloro-N,N-diphenyl-1,3,5-triazin-2-amine (3)

A solution of cyanuric chloride (100 mmol) in acetone (10 mL) was added slowly to an aqueous solution of NaHCO₃ (100 mmol) at -10 °C followed by diphenylamine (100 mmol) in acetone (10 mL) and stirred for 2 h. The white precipitate obtained was filtered and washed with cold water to remove unreacted cyanuric chloride and dried in vacuum. Column chromatography of the dried precipitate over silica gel using hexane and ethyl acetate (4:1) and drying under vacuum gave colorless crystals of **3** in 63% yield. mp 145 °C. IR (cm⁻¹): 3049, 1489, 1333, 1240. ¹H NMR (400 MHz, CDCl₃ δ ppm): 7.42-7.38 (m, 2H), 7.33-7.28 (m, 1H), 7.27-7.24 (m, 2H). ¹³C NMR (100 MHz, CDCl₃, δ ppm): 170, 165, 141, 129, 127, 124. ESI (m/z): 316.2 (M-1) Anal. Calcd. for C₁₅H₁₀Cl₂N₄ (Mw = 316. 17) C, 56.80; H, 3.18; Cl, 22.36; N, 17.66; found: C, 56.70; H, 3.10; Cl, 22.30; N, 17.60.

4,4'-(6-(diphenylamino)-1,3,5-triazine-2,4-diyl)bis(oxy)dibenzaldehyde (4)

A solution of 4-hydroxybenzaldehyde (20 mmol) in 10 mL of dichloromethane was treated with aqueous NaOH

(50 mL, 0.85 M) at room temperature followed by a solution of compound **3** (100 mmol) in dichloromethane (50 mL) and tetrabutylammonium bromide (TBAB) (20 mol %) was added slowly during 30 minutes. The mixture was stirred for 24 hours and the organic layer was separated and washed well with 10% NaOH, followed by distilled water. The resulting solution was dried with anhydrous Na₂SO₄ and the solvent was removed under vacuum and recrystallization from ethyl acetate to yield **4** as a colourless solid (Yield 63%). mp. 169 °C. IR(cm⁻¹): 1697, 1582, 1375, 1261. ¹H NMR (400 MHz, CDCl₃, δ ppm): 9.95(s, 1H), 7.80-7.77 (d, 2H), 7.28-7.24(m, 4H), 7.19-7.16 (m, 3H). ¹³C NMR (100 MHz, CDCl₃, δ ppm): 190, 171, 167, 156, 142, 133, 130, 129, 127, 126. ESI (m/z): 487.17(M-1), Anal. Calcd. for C₂₉H₂₀N₄O₄ (Mw =488.49) C, 71.30; H, 4.13; N, 11.47, Found: C, 71.20; H, 4.10; N, 11.37.

Synthesis of **5**

General procedure:- A mixture of aldehyde **4** (1 mmol) and of rhodanine-3-acetic acid/barbituric acid/thiobarbituric acid (22 mmol) and ammonium acetate (19 mmol) were dissolved in 0.5 M glacial acetic acid and heated at 120 °C for 12 h. After cooling, the precipitated target product was washed with chloroform and methanol to remove the unreacted reagents and starting materials.

DTOP-RHA (**5a**) Yellow powder. Yield 58%. IR(cm⁻¹): 3330, 1707, 1598, 1501, 1323, 1289. ¹H NMR (400 MHz, DMSO, δ ppm): 7.81 (s, 1H), 7.62-7.60 (d, 2H), 7.38-7.31 (m, 6H), 7.22 (m, 2H), 4.58 (s, 2H). ¹³C NMR (100 MHz, DMSO, δ ppm): 185, 171, 131, 128, 127, 122. Anal. Calcd for C₃₉H₂₆N₆O₈S₄ (Mw= 834.92). C, 56.10; H, 3.14; N, 10.07; S, 15.36; found: C, 56.05; H, 3.10; N, 9.97; S, 15.30.

DTOP-BA (**5b**) Yellow powder. Yield 68%. IR(cm⁻¹): 3325, 1603, 1390, 1115. ¹H NMR (400 MHz, DMSO, δ ppm): 11.23 (s, 1H), 11.10 (s, 1H), 10.79 (s, 1H), 8.30-8.21 (m, 4H), 7.31-6.88 (m, 5H). ¹³C NMR (100 MHz, DMSO, δ ppm): 163.0, 153.1, 150.1, 136.5, 132.6, 129.1, 127.7, 127.4. Anal. Calcd. for C₃₇H₂₄N₈O₈ (MW =740.77). C, 62.71; H, 3.41; N, 15.81; Found C, 62.65; H, 3.31; N, 15.75.

DTOP-TBA (**5c**) Yellow powder. Yield 66%. IR(cm⁻¹): 3460, 1655, 1546, 1364, 1209, 1152. ¹H NMR (400 MHz, DMSO, δ ppm): 12.36 (s, 1H), 12.25 (s, 1H), 8.16 (s, 1H), 8.13-8.11 (d, 2H) 7.29-7.22 (m, 6 H), 7.14-7.10 (m, 1H). ¹³C NMR (100 MHz, DMSO, δ ppm): 178, 170, 159, 154, 142, 135, 130, 128, 127, 122, 121, 118. Anal. Calcd. for C₃₇H₂₄N₈O₆S₂ (MW =708.64) C, 59.99; H, 3.27; N, 15.13; S, 8.66; found: C, 59.89; H, 3.20; N, 15.05; S, 8.60.

Electrochemical measurements

The electrochemical properties of the dyes were investigated by cyclic voltammetry (CV) and square wave voltammetry on a BAS 50W electrochemical workstation using a three electrode configuration. A glassy carbon electrode was used as the working electrode, platinum wire was used as the counter electrode and reference electrode used was Ag/AgCl. A 0.1 M DMF solution of *n*-Bu₄NPF₆ was used as the electrolyte. The solutions were saturated with argon prior to measurements. Ferrocene was used as a reference to standardize the measurements and the corrected values are reported against standard hydrogen electrode (SHE).

DSSC Fabrication and Characterization

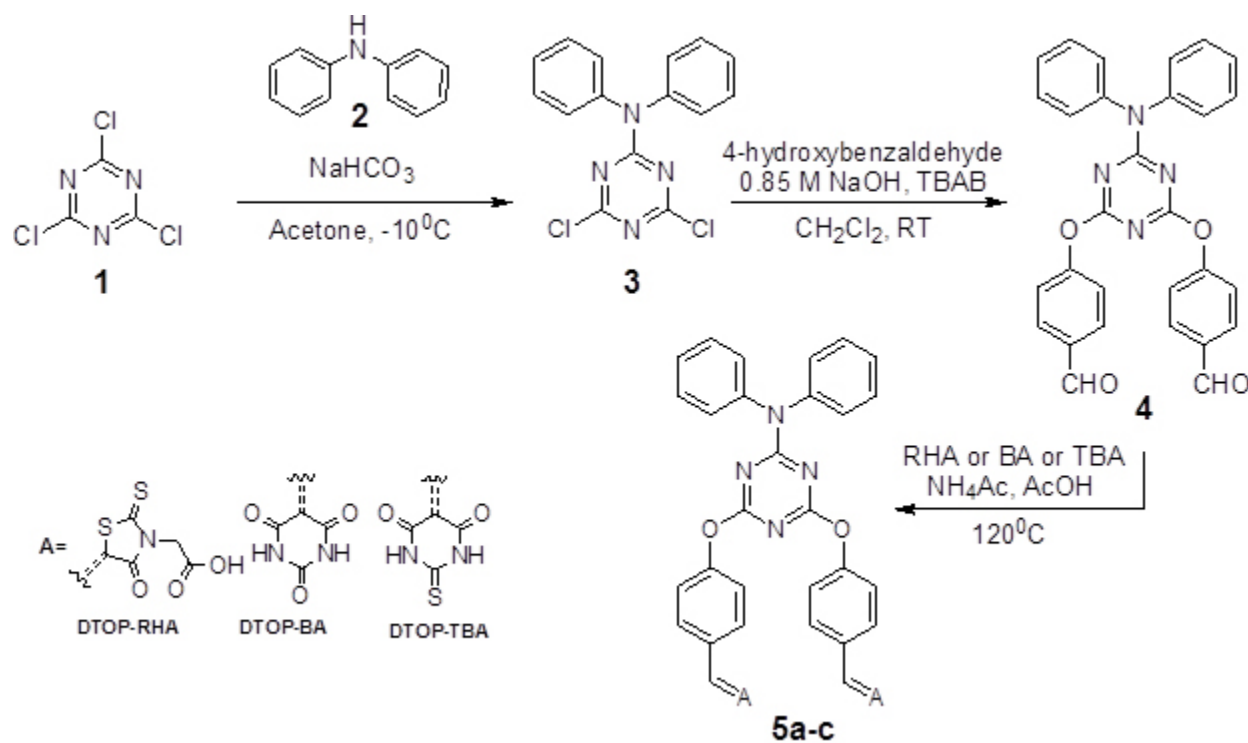
The photoelectrochemical properties of these dyes were studied by constructing photoelectrochemical cells using dye adsorbed TiO₂ as the photoanode, Pt coated Fluorine doped ITO as the cathode and I⁻/I₃⁻ containing LiI 0.4 M and 0.04 M I₂ in dried CH₃CN solution or Br⁻/Br₃⁻ LiBr 0.4 M, 0.04 M Br₂ in dry CH₃CN is used as the redox electrolyte. The preparation of the photoelectrodes and the fabrication of the DSSCs were carried out based on earlier reported methods [25]. The TiO₂ thin films were dipped in dye solution in DMF for 24 hours and washed successively with DMF, water and ethanol. Prior to measurements the cells were dried under vacuum in vacuum desiccators at room temperature. Dark and illuminated I-V characteristics of the cell were measured using a Keithley (2420C) Source Measure Unit. The cell was illuminated using a photo emission tech solar simulator. The photoanode was prepared by coating TiO₂ paste in a rectangular shape on the surface of FTO glass plate by doctor blade method followed by calcination at 450°C for 30 minutes. The TiO₂ electrodes were soaked in dye solution overnight and washed several times with DMF followed by methanol and dried. Pt coated FTO having drilled holes (1mm) for injecting appropriate electrolyte was used as the cathode. The dye coated electrode and the Pt counter electrode were assembled in a sealed sandwich model cell using meltonix as the binder. The active area of the cell was 0.16 cm² and the remaining area was masked with a black tape prior to characterization.

RESULTS & DISCUSSION

Design and Synthesis

We have made use of the ability of cyanuric chloride to undergo nucleophilic substitution reactions with amines and alcohols. All the chlorine atoms of cyanuric chloride can be substituted by primary amines or alcohols at room temperature or at slightly elevated temperatures. However, mono- substitution by nucleophiles requires low temperatures and in the present synthesis mono-substitution by diphenylamine was ensured by carrying

out the reaction at $-10\text{ }^{\circ}\text{C}$ using NaHCO_3 as a base. The remaining chlorine atoms were substituted successfully at room temperature by the *in situ* generated phenoxide anion of 4-hydroxybenzaldehyde with 10% NaOH in dichloromethane in the presence of a phase transfer catalyst tetrabutylammonium bromide. The dialdehyde was made to react with two equivalents of rhodanine acetic acid, barbituric acid or thiobarbituric acid to produce the corresponding D- π -A type triads. All these were soluble in DMF and DMSO. Moderate solubility was observed in methanol and in acetonitrile. DMF was used as the solvent for photophysical as well as electrochemical studies.



Scheme 2. Synthetic Route for the dyes 5a-c

Photophysical studies

Absorption spectra of all dyes show characteristic charge transfer absorption bands around 370 nm , with onset of absorption extending to 450 nm (dark line in Figure 1a-c). The diffuse reflectance spectra of all the compounds in the powder form however show broad absorption spectra peaking at 400 nm and the onset of absorption extending to 500 nm (cf. supplementary data). This red shift could be due to the stacking arrangement that facilitate intramolecular charge transfer [26].

The ability of these dyes in binding with TiO_2 was probed by adding colloidal TiO_2 prepared in aqueous acetic acid medium to the dye solution in DMF. The absorption spectra of DTOP-RHA and DTOP-BA did not show any change upon addition of colloidal TiO_2 . However, DTOP-TBA showed a decrease in the absorbance at 372 nm . This could be due to protonation of the oxa- bridge followed by nucleophilic displacement of the acceptor unit by hydroxyl anions in the colloidal TiO_2 solution. Nano-crystalline TiO_2 thin films were made from a paste of TiO_2 by doctor blading and annealing at $500\text{ }^{\circ}\text{C}$

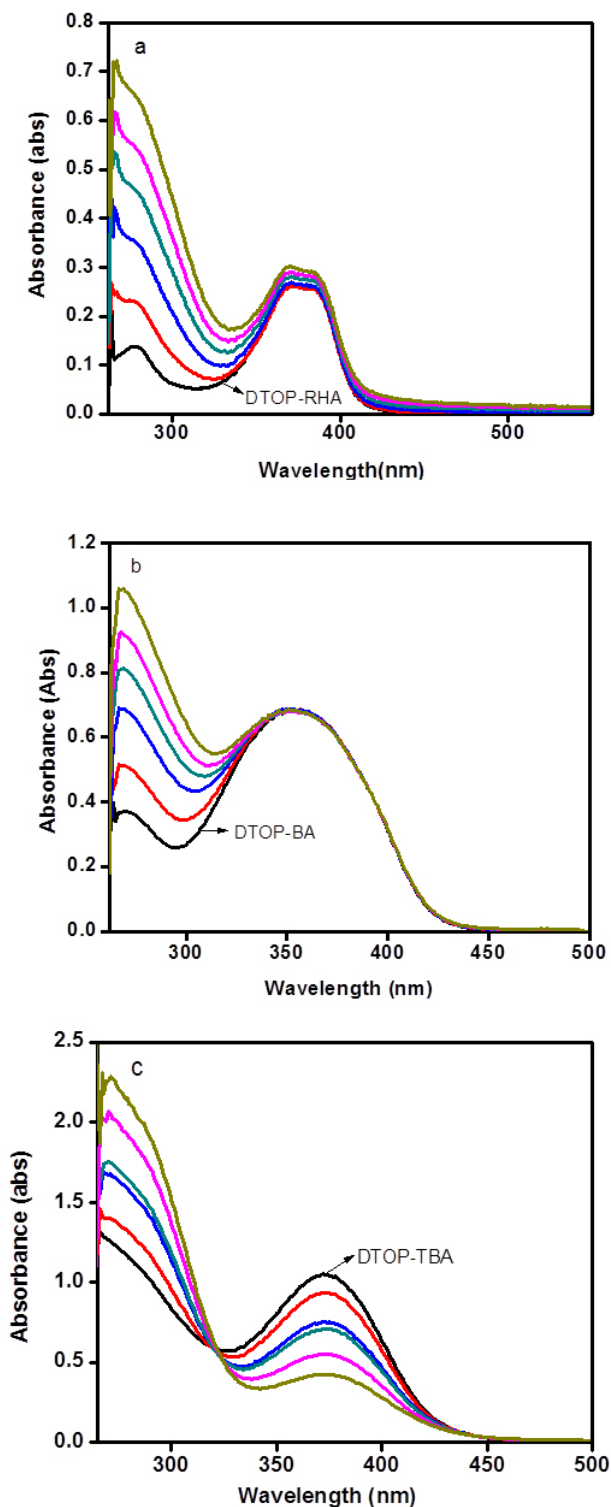


Fig 1. Comparison of the UV-Visible absorption spectrum of dyes a) DTOP-RHA, b) DTOP-BA, c) DTOP-TBA in DMF solution (dark line) and in the presence of increasing amounts of colloidal TiO₂ (10 – 300 μM).

for 30 minutes in a muffle furnace and dye coated TiO₂ thin films were prepared immersing these thin films in respective dye solutions in DMF for 24 h. All films showed light yellow color and attempts to get diffuse reflectance spectra were not successful due to high reflectance of the thin films. Figure 1 shows a comparison of the absorption spectrum of the dyes in DMF solution and the spectrum obtained at different concentrations of colloidal TiO₂. In order to determine the singlet excited state energy of these dyes fluorescence emission spectra were obtained by exciting the dye solutions in DMF at 370 nm (Figure 2). The singlet excitation energy E_{0-0} was calculated from the point of intersection of the normalized absorption and emission spectra of each dye. Photophysical properties of all the dyes were summarized in Table 1.

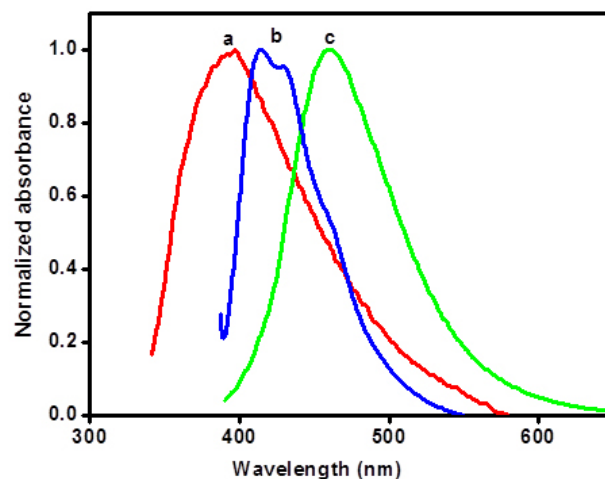


Fig 2. Fluorescence spectra of compounds DTOP-BA (a), DTOP-TBA (b) and DTOP-RHA (c) in DMF ($\sim 1 \times 10^{-8}$ M, $\lambda_{ex} = 370$ nm).

Electrochemical Properties

The oxidation potentials of these dyes were determined from the square wave voltammograms (cf. supplementary data) of these dyes. They exhibit characteristic oxidation potentials at 1.26, 1.26 and 1.22 V respectively vs. NHE [27]. The results are summarized in Table 2. These values are lower than the redox potential of redox couples I⁻/I₃⁻ and Br⁻/Br₃⁻ the common redox couples used in the construction of DSSC's. The energy gap between the redox couple and oxidation potential of the dye is significant in determining the current as well as the fill factor. For the dyes used in the present study the energy gap obtained is very large for I⁻/I₃⁻ (0.53 vs NHE) is 0.73 V in comparison

to Br⁻/Br₃⁻ (1.09 V vs NHE) which is 0.17 V which makes the regeneration of the oxidized dye thermodynamically favorable during the operation of the cell [28]. The HOMO and the LUMO energies of these dyes referenced to NHE were calculated from the oxidation potentials of these dyes

and their respective singlet energy. Estimations of HOMO and LUMO energies against vacuum continuum were also been made and all the values are presented in Table 2 [29-30].

Table 1. Photophysical properties of DTOP-RHA, DTOP-BA and DTOP-TBA in DMF.

Dyes	λ_{\max} (Abs) nm	ϵ_{\max} dm ³ mol ⁻¹ cm ⁻¹	λ_{\max} (Em) nm	E _{0,0} eV	E _{ox} V vs. SHE
DTOP-RHA	370 390*	2.55 × 10 ³	430	3.04	1.26
DTOP-BA	373 375*	2.18 × 10 ³	405	3.1	1.26
DTOP-TBA	375 380*	2.3 × 10 ³	405, 429	3.06	1.22

Table 2. Electrochemical properties and band gaps of DTOP-RHA, DTOP-BA and DTOP-TBA in DMF.

Dyes	E _{on set} in DMF	E _{onset (ox)} Vs E _{FOC} /V	E(S+/S) vs NHE/ V	E ₀₋₀ (eV)	LUMO vs NHE/eV	E _{gap} / V	HOMO(IP)/eV	LUMO (EA)/eV
DTOP-RHA	1.17	1.06	1.26	3.04	-1.78	1.28	-6.06	-2.98
DTOP-BA	1.17	1.06	1.26	3.1	-1.84	1.34	-6.06	-2.96
DTOP-TBA	1.13	1.02	1.22	3.04	-1.82	1.32	-6.02	-2.98

E_{FOC} = -0.11 V vs. Ag/AgCl the ground-state oxidation potentials E(S+/S) (HOMO) were measured in DMF containing 0.1 M tetrabutylammonium hexafluorophosphate as supporting electrolyte using a glassy carbon working electrode, a Pt counter electrode and a Ag/AgCl reference electrode; the E₀₋₀ value was estimated from the cross-section of absorption and emission spectra; E_{gap} is the energy gap between LUMO of the dye and the conduction band level of TiO₂ (-0.5 V vs. NHE); ionization potential: IP = - 4.8 - (E_{onset (ox)} - E_{FOC}); electron affinity: EA - E₀₋₀ = IP

Theoretical Study

The optimized geometry of the dyes as well as the frontier orbitals and their energies are computed by density functional theory (DFT) with B3LYP exchange-correlation functional [31, 32] and 6-31+G(d) basis set. The stationary points are characterized by frequency calculation. To include the effects of solvation the polarization continuum model (PCM) for DMF has been used in the calculations. All calculations were performed with the GAUSSIAN09 quantum chemistry package. The calculations were repeated with B3P86 functional and

found no significant variation in the geometry and orbital energies obtained by B3LYP functional correlated well with the experimental data (Table 3). The optimized geometry along with the frontier orbital representation and their respective energies against vacuum continuum is given in Figures 3. Contrary to our expectation the orbital coefficients of the HOMO for all compounds were found to be delocalized over the triazine core which is one of the acceptor units. This delocalization extends over the terminal rhodanine-3-acetic acid acceptor unit in the case of the dye DTOP-RHA. Delocalization of HOMO over the triazine has a profound effect in the lowering of HOMO energies as well as on the observed oxidation potential of all the dyes. Both electrochemical and theoretical data suggests that they are difficult to oxidize in comparison to oxidation of diphenylamine. This also explains the higher excitation energy and thus lower coverage of the solar spectrum in the visible region. The dyes DTOP-BA and DTOP-TBA show better directionality of charge transfer as the HOMO and LUMO are localized on different regions of the molecule. This effect is evident in the more red shifted absorption spectrum obtained for these dyes. The theoretically calculated energy levels are also found to be matching with the experimental values obtained from

electrochemical measurements. The utility of these dyes in the fabrication of DSSCs was assessed by comparing the redox levels of the dyes, redox electrolytes and the TiO₂ photoanode. Figure 4 illustrates this comparison and it is

evident that the electron injection by the excited dye to the TiO₂ photoanode and the regeneration of the dye by the redox electrolyte are exergonic.

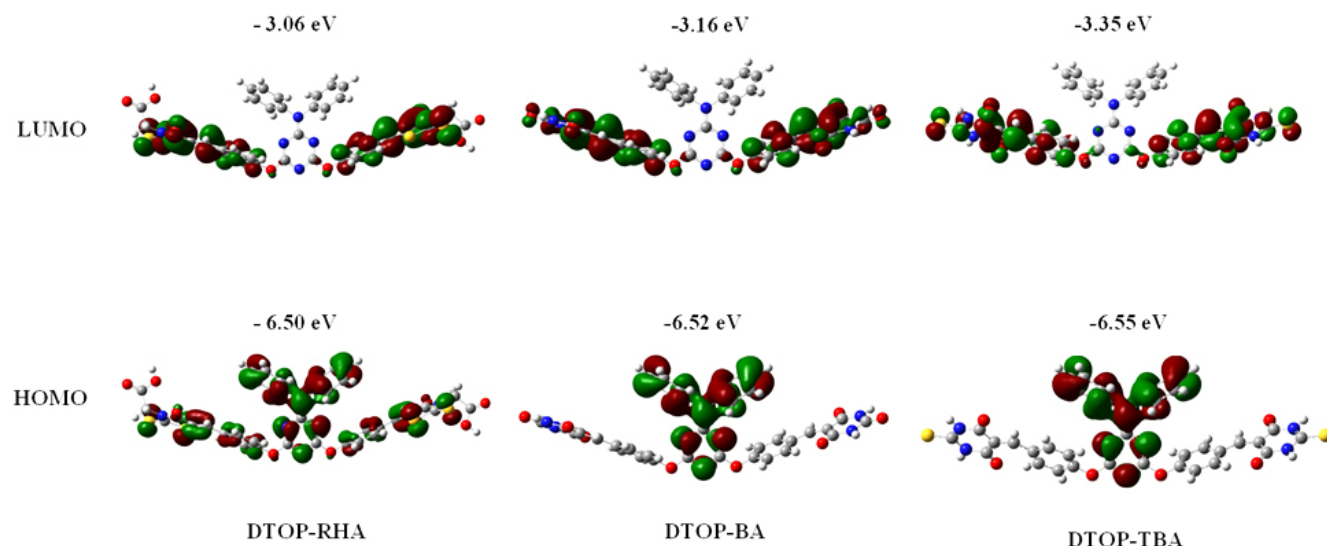


Fig 3. Optimized geometries of the dyes computed using DFT theory at the B3LYP/6-31G level

Table 3. Comparison of theoretically and experimentally determined energies of HOMO and LUMO orbitals of dyes DTOP-RHA, DTOP-BA and DTOP-TBA. (Values in parenthesis are those obtained for B3P86 functional.)

Dyes	Experimental		Theoretical (DFT-B3LYP)	
	HOMO (V)	LUMO(V)	HOMO (V)	LUMO (V)
DTOP-RHA	-6.64	-3.05	-6.50 (-7.15)	-3.06, (-3.70)
DTOP-BA	-6.63	-3.53	-6.52 (-7.16)	-3.16 (-3.80)
DTOP-TBA	-6.50	-3.64	-6.55 (-7.20)	-3.35 (-3.99)

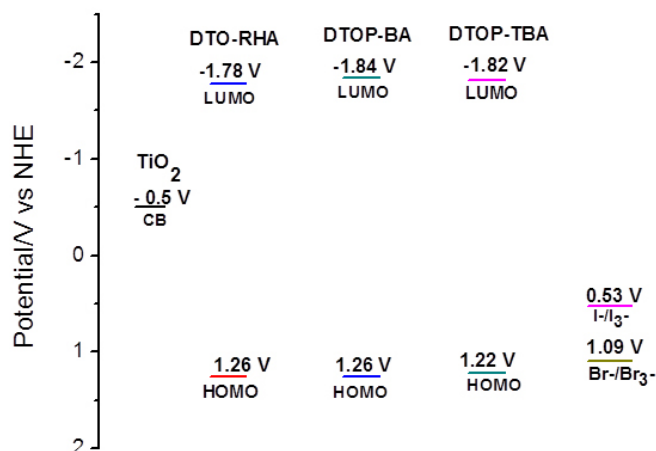


Fig 4. Schematic energy level diagram for a DSSC based on dyes attached to nanocrystalline TiO₂ film deposited on conducting FTO.

Photoelectrochemical Properties

Under illumination by a 1.5 AM light source all the cells constructed gave I-V characteristics for typical photodiodes. A few representative J-V curves obtained for dyes DTOP-RHA, DTOP-BA and DTOP-TBA when Br⁻/Br₃⁻ was used as the electrolyte are given in Figure 5. The solar cell parameters obtained from the photocurrent measurements were summarized in Table 4. The solar energy to electrical energy conversion efficiency was calculated from Open circuit voltage, short-circuited current, fill factor and the incident photon flux (P_{in}) by using equation,

$$\eta = \frac{J_{sc} V_{oc} FF}{P_{in}} \quad (\text{Eq. 1})$$

Under our experimental conditions an efficiency of 3 % was obtained for the N719 dye when I⁻/I₃⁻ was used as the electrolyte. The results show that the observed conversion efficiency are lower and are in the range of 0.01 – 0.06 where the cell made from the dye DTOP-TBA with Br⁻/Br₃⁻ was found to be the most efficient in the series. The data obtained for the cells with I⁻/I₃⁻ as the electrolyte were very low in comparison to the data obtained for Br⁻/Br₃⁻ in terms of Voc and thus η. This could be due to the low potential difference between the Fermi level and the high lying redox potential of I⁻/I₃⁻ in comparison to Br⁻/Br₃⁻. The poor efficiency data observed could be due to a combined effect of lower coverage of the solar spectrum by the dyes as well as lower binding coefficients. Relatively better performance of DTOP-TBA may be the result of the high lying HOMO making regeneration of the dye efficient in comparison to other dyes. Based on a similar design strategy better performing dye sensitizers can be synthesized by incorporating better donor groups and by incorporating groups that enhance conjugation at the acceptor site.

Table 4. DSSC Performance data of the dyes

Dyes	J _{sc} , mA cm ⁻²	V _{oc} , mV	FF, %	η, %
DTOP-RHA	-0.160 ^a (0.001)	0.273 ^a (0.001)	45 ^a (3.78)	0.02 ^a (0.002)
	-0.078 ^b (0.006)	0.477 ^b (0.007)	79 ^b (6.65)	0.03 ^b (0.0007)
DTOP-BA	-0.094 ^a (0.001)	0.210 ^a (0.002)	50 ^a (1.5)	0.01 ^a (0.0004)
	-0.124 ^b (0.005)	0.580 ^b (0.004)	62 ^b (2.0)	0.04 ^b (0.0005)
DTOP-TBA	-0.129 ^a (0.005)	0.182 ^a (0.008)	42 ^a (5.29)	0.01 ^a (0.0005)
	-0.215 ^b (0.00)	0.475 ^b (0.004)	58 ^b (3.5)	0.06 ^b (0.0004)

a* I⁻/I₃⁻ electrolyte. b* Br⁻/Br₃⁻ electrolyte

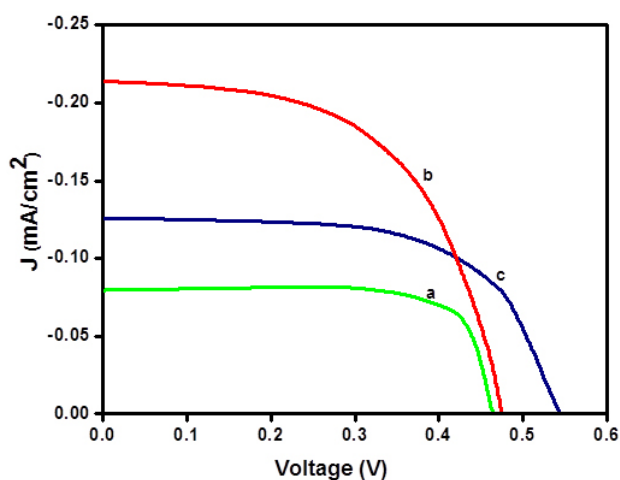


Fig 5. Photocurrent density–voltage curves of the compounds DTP-RHA (a), DTP-BA (b) and DTP-TBA (c) using Br⁻/Br₃⁻ electrolyte

CONCLUSION

We have designed and synthesized three novel D-π-A-A systems with triazine core as the non-conjugating spacer/acceptor with rhodanine-3-acetic acid (DTOP-RHA), barbituric acid (DTOP-BA) or thiobarbituric acid (DTOP-TBA) as anchoring acceptor groups. Electrochemical, photophysical studies and theoretical studies show that they have suitable properties for use as dyes in dye sensitized solar cells. The applicability of these dyes for the DSSC was tested by constructing the sandwich model cell. However, the observed efficiency was lower than that obtained for N719 dye under similar experimental conditions. This is attributed to the low coverage of the solar spectrum and large energy gap between the LUMO of the dyes and the conduction band of the TiO₂.

The results suggest tuning of the LUMO energy by incorporating additional conjugating groups in the acceptor side of the design. Further studies in this direction are progressing.

REFERENCES

1. Sarah, K.; Keith E., National Renewable Energy Laboratory (NREL), Golden, CO, February 2016, https://en.wikipedia.org/wiki/Solar_cell
2. Seo, J.; Noh, J. H.; Seok, S. I., *Acc. Chem. Res.* **2016**, *49*, 562–572.
3. Hagfeldt, A.; Graetzel, M., *Chem. Rev.* **1995**, *95*, 49–68.
4. Do, K.; Choi, H.; Lim, K.; Jo, H.; Cho, J. W.; Nazeeruddin, M. K.; Ko, J., *Chem. Commun.* **2014**, *50*, 10971–10974.
5. Liu, J.; Wang, K.; Zhang, X.; Li, C.; You, X., *Tetrahedron.* **2013**, *69*, 190–200.
6. Ning, Z.; Tian, H., *Chem. Commun.* **2009**, 5483–5495.
7. Ooyama, Y.; Harima, Y., *Eu. J. Org. Chem.* **2009**, 2903–2934.
8. Sharma, G. D.; Angaridis, P. A.; Pipou, S.; Zervaki, G. E.; Nikolaou, V.; Misra, R.; Coutsolelos, A. G., *Org. Electron.* **2015**, *25*, 295–307.
9. Zervaki, G. E.; Roy, M. S.; Panda, M. K.; Angaridis, P. A.; Chrissos, E.; Sharma, G. D.; Coutsolelos, A. G., *Inorg. Chem.* **2013**, *52*, 9813–9825
10. Bella, F.; Gerbaldi, C.; Barolo, C.; Gratzel, M., *Chem. Soc. Rev.* **2015**, *44*, 3431–3473.
11. Grätzel, M., *Nature.* **2001**, *414*, 338–344.
12. Nazeeruddin, M. K.; Pechy, P.; Renouard, T.; Zakeeruddin, S. M.; Humphry-Baker, R.; Comte, P.; Liska, P.; Cevey, L.; Costa, E.; Shklover, V.; Spiccia, L.; Deacon, G. B.; Bignozzi, C. A.; Gratzel, M., *J. Am. Chem. Soc.* **2001**, *123*, 1613–1624.
13. Nazeeruddin, M. K.; Zakeeruddin, S. M.; Humphry-Baker, R.; Jirousek, M.; Liska, P.; Vlachopoulos, N.; Shklover, V.; Fischer, C. H.; Gratzel, M., *Inorg. Chem.* **1999**, *38*, 6298–6305.
14. Hwang, S.; Lee, J. H.; Park, C.; Lee, H.; Kim, C.; Park, C.; Lee, M.-H.; Lee, W.; Park, J.; Kim, K.; Park, N.-G.; Kim, C., *Chem. Commun.* **2007**, 4887–4889.
15. Xu, M.; Li, R.; Pootrakulchote, N.; Shi, D.; Guo, J.; Yi, Z.; Zakeeruddin, S. M.; Graetzel, M.; Wang, P., *J. Phys. Chem. C.* **2008**, *112*, 19770–19776.
16. Sayama, K.; Hara, K.; Mori, N.; Satsuki, M.; Suga, S.; Tsukagoshi, S.; Abe, Y.; Sugihara, H.; Arakawa, H., *Chem. Commun.* **2000**, 1173–1174.
17. Hara, K.; Sayama, K.; Ohga, Y.; Shinpo, A.; Suga, S.; Arakawa, H., *Chem. Commun.* **2001**, 569–570.
18. Horiuchi, T.; Miura, H.; Sumioka, K.; Uchida, S., *J. Am. Chem. Soc.* **2004**, *126*, 12218–12219.
19. Wang, Z.-S.; Koumura, N.; Cui, Y.; Takahashi, M.; Sekiguchi, H.; Mori, A.; Kubo, T.; Furube, A.; Hara, K., *Chem. Mater.* **2008**, *20*, 3993–4003.
20. Song, J.-L.; Amaladass, P.; Wen, S.-H.; Pasunooti, K. K.; Li, A.; Yu, Y.-L.; Wang, X.; Deng, W.-Q.; Liu, X.-W., *New J. Chem.* **2011**, *35*, 127.
21. Wu, Y.; Zhu, W., *Chem. Soc. Rev.* **2013**, *42*, 2039–2058.
22. Zhong, H.; Xu, E.; Zeng, D.; Du, J.; Sun, J.; Ren, S.; Jiang, B.; Fang, Q., *Org. Lett.* **2008**, *10*, 709–712.
23. Suneesh, C. V.; Vinayak, M. V.; Gopidas, K. R., *J. Phys. Chem. C.* **2010**, *114*, 18736–18744.
24. Suneesh, C. V.; Gopidas, K. R., *J. Phys. Chem. C.* **2010**, *114*, 18725–18734.
25. Zervaki, G. E.; Roy, M. S.; Panda, M. K.; Angaridis, P. A.; Chrissos, E.; Sharma, G. D.; Coutsolelos, A. G. *Inorg. Chem.* **2013**, *52*, 9813–9825.
26. Zhong, H.; Lai, H.; Fang, Q., *J. Phys. Chem. C.* **2011**, *115*, 2423–2427.
27. Neil, G.; William, E. G., *Chem. Rev.* **1996**, *96*, 877–910.
28. Wang, Z. S.; Sayama, K.; Sugihara, H., *J. Phys. Chem. B.* **2005**, *109*, 22449–22455.
29. Xie, Q. J.; Kuwabata, S.; Yoneyama, H., *J. Electroanal. Chem.* **1997**, *420*, 219–225.
30. Fermin, D. J.; Teuel, H.; Scharaifker, B. R., *J. Electroanal. Chem.* **1996**, *401*, 207–214.
31. Lee, C.; Yang, W.; Parr, R. G., *Phys. Rev. B.* **1988**, *37*, 785–789.
32. Becke, A. D., *J. Chem. Phys.* **1993**, *98*, 5648–5652.